Available online at www.sciencedirect.com
SCIENCE DIRECT®
Journal of Catalysis 236 (2005) 1–8
JOURNAL OF CATALYSIS
www.elsevier.com/locate/jcat

DFT and ATR-IR insight into the conformational flexibility of cinchonidine adsorbed on platinum: Proton exchange with metal

Angelo Vargas, Davide Ferri, Alfons Baiker *

Department of Chemistry and Applied Biosciences, Swiss Federal Institute of Technology, ETH-Hönggerberg, CH-8093 Zurich, Switzerland

Received 15 July 2005; revised 19 August 2005; accepted 2 September 2005

Available online 7 October 2005

Abstract

The adsorption mode of cinchonidine on platinum is discussed in the light of new computational studies in which the alkaloid is adsorbed on a large metal cluster. Previous computations focused on the role of 1(S)-(4-quinolinyl)ethanol as anchoring group, but in the present study the role of the quinuclidine ring is analyzed, leading to a consistent view of the roles of both moieties of the alkaloid in the adsorption process. The tertiary nitrogen of the quinuclidine moiety can participate in the anchoring of the alkaloid and can be protonated by surface hydrogen. The conformational flexibility of the quinuclidine moiety was investigated by attenuated total reflection infrared experiments under nearly in situ conditions, by comparing the adsorption behavior of cinchonidine and *O*-phenyl-cinchonidine on platinum. Close agreement was found between experimental observations and theoretical calculations. A mechanism is proposed whereby the tertiary nitrogen can promote charge polarization of hydrogen and its transfer to the substrate.

Keywords: Cinchonidine; Adsorption; DFT; Platinum; Enantioselective hydrogenation; In situ; ATR-IR spectroscopy; Proton exchange

1. Introduction

The enantioselective hydrogenation of activated ketones on cinchona alkaloid-modified platinum [1–3] is the most well studied heterogeneous asymmetric catalytic system [4,5]. The advantages inherent to heterogeneous catalysis are combined with high reaction rates and enantioselectivities. Substrates in which the keto-carbonyl has been successfully asymmetrically hydrogenated using this catalyst are linear and cyclic α-ketoesters [6–10], α-diketones [11–15], α-ketoacetals [16,17], α,α,α-trifluoroketones [18–22], and linear and cyclic α-ketoamides [23–25]. Palladium also can be similarly modified using this technique, leading to effective enantioselective hydrogenation of C=C double bonds in 2-pyrones [26,27], furan and benzofurancarboxylic acids [28] and enol esters [29]. The study of the mechanism of interaction among the surface, the substrate, and cinchonidine (CD) is a necessary step toward tailoring catalysts that work using the principle of chiral surface modification. Virtually all of the literature on this subject agrees that the quinoline moiety of the alkaloid acts as an anchoring group to bind the modifier to the metal, and that this adsorption generates chiral sites able to discriminate between the pro-*R* and pro-*S* faces of a prochiral ketone [1–3]. The enantiodiscriminating features of such chiral sites can be reproduced in tailored modifiers that imitate the main functions of the alkaloids [30] and can even be changed, thus inverting the absolute configuration of the alcohol ultimately obtained, by chemical modification of the surface modifier [31]. In some cases the enantiodiscriminating properties of the catalyst can be dynamically switched by using modifiers that have the dual feature of competing for adsorption and generating sites of opposite enantioselectivity [32]. This variety of features makes this reaction system unique within heterogeneous catalysis, but extensive control of its catalytic behavior can be achieved only via detailed knowledge of the structure and activity of the surface chiral sites. To date, our research strategy has involved the combination of three aspects: phenomenological observations, structural-spectroscopic studies, and computational studies. The first of these includes the study of catalytic behavior under various conditions (e.g., pressure, concentration, temper-

* Corresponding author.
E-mail address: baiker@tech.chem.ethz.ch (A. Baiker).

0021-9517/$ – see front matter
doi:10.1016/j.jcat.2005.09.009

ature, solvent). In addition, new substrates and the study of their optimal behavior are contemplated by this approach [2,3,30]. The second approach aims to collect structural information on the solid-liquid interface by probing a model metal catalyst using attenuated total reflection infrared (ATR-IR) spectroscopy. The high surface sensitivity of this technique allows it to provide close to in situ structural information on the modified surface [33,34]. Finally, the third approach aims to obtain submolecular structural information and generates a consistent synthesis of the results obtained with the other two methods. This is achieved by means of state-of-the-art density functional calculations of large platinum clusters used as models for the metal surface [35,36]. Unlike as in our previous study, in which we mainly analyzed the adsorption behavior of the quinoline moiety [35,36], here we discuss the contribution of the quinuclidine moiety. This allows a more complete and detailed description of the adsorption mode and conformation of the surface modifier. Furthermore, we discuss the problem of the hydrogen transfer from the surface to the substrate in proximity of the chiral space generated by the modifier and set forth a new hypothesis on the mechanism of hydrogen transfer in aprotic solvents.

2. Methods

2.1. Computational methods

The adsorption studies were performed using the two platinum clusters shown in Fig. 1 formed by 38 (a) and 25 (b) platinum atoms, the former used to minimize edge effects and the latter used to reduce computation times, as explained in the Results section. The smaller cluster was generated from the larger one by setting 13 atoms as dummies (Fig. 1b). All of the cluster calculations were performed using the Amsterdam Density Functional program package [37]. The spin state of the Pt 38 cluster was optimized, obtaining the optimal difference between α and β electrons (α–β) equal to 10. The spin state of the Pt 25 cluster was optimized with a hydrogen atom adsorbed, for which the system-optimal α–β is 3. Fig. 2 shows the dependence of the energy from the spin state in the two cases. All adsorption studies were performed using these optimized values. A frozen core approximation was used for the inner core of all atoms. The orbitals up to 1s were kept frozen for all second-row elements, and orbitals up to 4f were kept frozen for platinum. Decreasing the Pt frozen core to 4d, implying the explicit calculation of 14 additional electrons per platinum atom, has been shown to increase the adsorption energy for the adsorption of benzene by only about 5 kJ/mol [38]. The importance of relativistic effects for calculations involving platinum has been demonstrated previously [39,40]. The core was modeled using a relativistically corrected core potential created with the DIRAC utility in the ADF program. The DIRAC calculations imply the local density functional in its simple X-α approximation without any gradient corrections, but the fully relativistic Hamiltonian was used, including spin-orbit coupling. It was found that the scalar relativistic correction could account for up to 70% of the total energy in the adsorption of carbon monoxide on platinum, and that the calculated adsorption site was also influenced by using a relativistic correction [39]. Thus the relativistic scalar approximation (mass velocity and Darwin corrections) was used for the Hamiltonian with the zero-order regular approximation (ZORA) method [41], in which spin orbit coupling is included already in zero order. The first-order Pauli formalism [42] was shown to have theoretical deficiencies due to the behavior of the Pauli Hamiltonian at the nucleus, which led to variational collapse [43] for increasing basis set size. The ZORA formalism requires a special basis set that includes much steeper core-like functions implemented in the code. Within this basis set, the double-ζ (DZ) basis functions were used for platinum, and double-ζ plus polarization (DZP) basis functions were used for the second-row elements. The local part of the exchange and correlation functional was modeled using a Vosko et al. [44] parameterization of the electron gas. The nonlocal part of the functional was modeled using the Becke correction [45] for the exchange and the Perdew correction [46] for the correlation. Energies of surface conformers were compared by taking the difference between the total electronic energies of the calculated structures. All calculations were run unrestricted. The bond distance for the platinum was fixed to the experimental

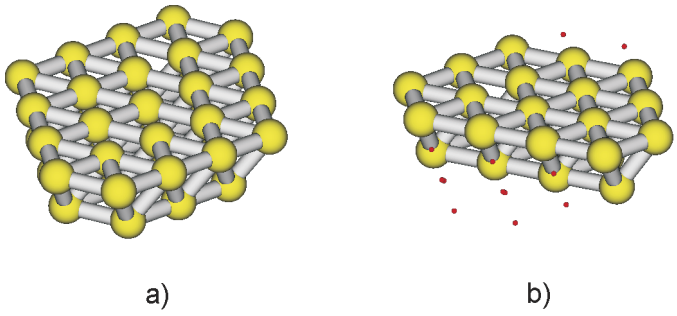

Fig. 1. The Pt 38 (a) and Pt 25 (b) clusters used for simulation of a platinum surface.

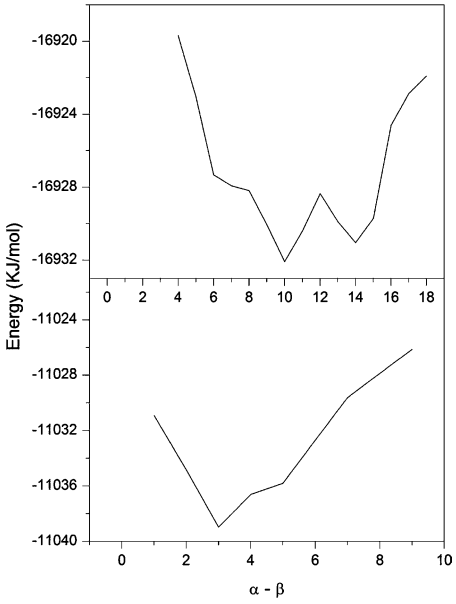

Fig. 2. Dependence of energy on spin state for the Pt 38 cluster (top) and for the Pt 25 cluster with hydrogen adsorbed (bottom).

value of 2.775 Å for bulk metal [47]. Molden [48] was used as graphical interface.

2.2. ATR-IR spectroscopy

Model films of 1 nm Pt on 100 nm Al_2O_3 were prepared by electron beam physical vapour deposition on a Ge internal reflection element, as described previously [49]. After deposition, the coated crystal was transferred to the ATR-IR cell, which was then placed on a commercial mirror setting within the sample compartment of the IR spectrometer (IFS 66, Brucker Optics). After purging overnight with dry air to minimize contribution from atmospheric water vapour and CO_2, the temperature of the cell was set to 15 °C, and a spectrum of the dry Pt/Al_2O_3 film was acquired before admitting N_2-saturated CH_2Cl_2 through the cell from a glass bubble tank. N_2 was then replaced by H_2 in the same tank while the solution was being continuously pumped to the cell. The hydrogen treatment is required to obtain domains of clean and reduced Pt [49,50]. At this point, a H_2-saturated solution of the chiral modifier ($C = 0.1$ mM) was admitted to the cell from a second glass bubble tank to follow adsorption. Either H_2-saturated CH_2Cl_2 or an H_2-saturated solution of a second modifier was then pumped across the Pt/Al_2O_3 film to monitor for signals due to strongly adsorbed species [32]. Spectra were collected throughout the experiment by co-adding 200 scans at 4 cm^{-1} resolution and were rationed against the last spectrum during the H_2-treatment. Cinchonidine (Fluka; 98%), cinchonidine hydrochloride (Fluka), and *O*-phenyl-cinchonidine (Ubichem; 99.5%) were used as received.

3. Results

3.1. Conformations of cinchonidine on the surface

The study of the adsorption of the anchoring group of CD 1(S)-(4-quinolinyl)ethanol (QUE) on platinum showed that optimum adsorption was reached when all carbon atoms and the quinoline nitrogen were interacting with platinum [35]. In the present work the use of larger platinum clusters allowed us to calculate the interaction of the whole alkaloid with the metal and thus completes our view of the constraints set by the surface to the conformational flexibility of the quinuclidine moiety. This is an important issue because the most accredited model for this reaction [2,4,8] postulates an interaction between the quinuclidine tertiary nitrogen and the incoming substrate via a hydrogen bond with the quinuclidine ring. This interaction has been interpreted as the critical one for rate acceleration and generation of an enantiomeric excess [51–53], and its existence has been supported by spectroscopic evidence [54].

Fig. 3 shows the 2 degrees of freedom τ_1 and τ_2 of CD, through which its conformational complexity has been extensively described in vacuum and in solution [55–57]. It was previously noted [35] that when CD is adsorbed via the quinoline ring, rotation around the C(4′)–C(9) bond leads to the decreasing of the distance of the quinuclidine moiety from the metal (Fig. 4). It also has been observed [35] that this approach to the surface is consistent with the rapid hydrogenation of the

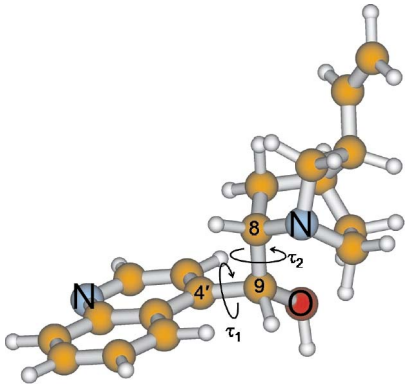

Fig. 3. Cinchonidine in the Open(3) conformation. Angles τ_1 and τ_2 define the relative positions of the two main moieties of the alkaloid.

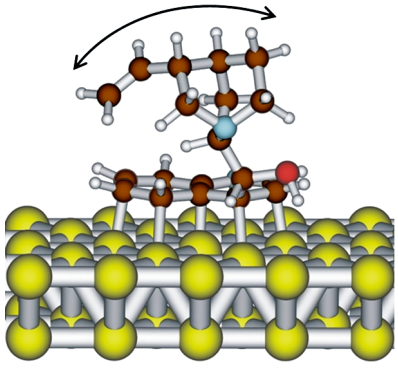

Fig. 4. Adsorption of CD on platinum based on the calculated adsorption of the anchoring group 1(S)-(4-quinolinyl)ethanol. The rotational angles τ_1 and τ_2 (Fig. 3) are the degrees of freedom that account for the conformational flexibility of the alkaloid.

C(10)=C(11) double bond, occurring experimentally within the first few minutes after the start of the reaction [58]. Fig. 4, based on cluster calculations from our previous work [35], was obtained not by complete optimization of the alkaloid on the metal, but rather by separate optimization of the anchoring group and then of the quinuclidine moiety at different levels of theory. This procedure was used to make the computation feasible.

In the present work we could instead use the same level of theory to calculate the entire alkaloid on a cluster of 38 platinum atoms and study the effect of the rotations about the angles τ_1 and τ_2, therefore addressing the problem of the conformational analysis of the adsorbed alkaloid. Fig. 5 shows the adsorption modes surface open(4) [SO(4); Figs. 5a–b] and surface open(3) [SO(3); Figs. 4c–d]. These names derive from the close resemblance to the open(3) and open(4) conformations found in vacuum and in solution [35,55–57]. SO(3) is more stable than SO(4) by 9.2 kJ/mol at this level of theory (Table 1). Both surface conformations allow for rotation around the angle τ_2, so that the tertiary nitrogen can form a σ bond to the metal surface. This rotation generates the conformations shown in Fig. 6. These two conformations are termed surface quinuclidine bound(1) [SQB(1); Figs. 6a–b] and surface quinuclidine bound(2) [SQB(2); Figs. 6c–d]. SQB(1) is 15.5 kJ/mol more stable than SO(4), whereas SQB(2) is 20.5 kJ/mol less stable

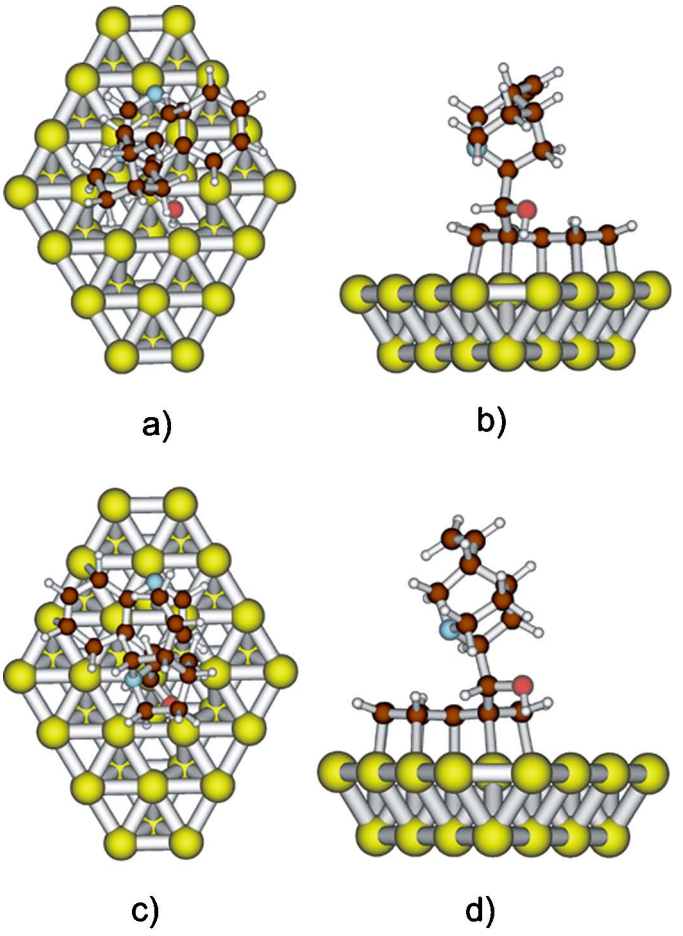

Fig. 5. Adsorption of CD on a Pt 38 cluster. Top and side views of Surface Open(4) (SO(4)) (a–b) and Surface Open(3) (SO(3)) (c–d). The quinuclidine moiety is detached from the metal and does not contribute to the anchoring of the alkaloid.

Table 1
Relative energies of the surface conformations

Conformation	SO(4)	SO(3)	SQB(1)	SQB(2)
Energy (kJ/mol)	15.5	6.3	0	26.8

SO(4) refers to Figs. 5a and b. SO(3) refers to Figs. 5c and d. SQB(1) refers to Figs. 6a and b. SQB(2) refers to Figs. 6c and d. Zero value is set to the lowest energy structure.

than SO(3). Table 1 summarizes the relative energies of these surface conformations, taking as zero the energy of the most stable surface conformer.

3.2. Hydrogen uptake from the surface

The structures in Fig. 6 were obtained for a clean surface, but the catalyst obviously is active only in presence of surface hydrogen. Therefore, we investigated the consequences of exposing the quinuclidine moiety to surface hydrogen.

First, a hydrogen atom was adsorbed on the Pt 25 cluster. For this system, the optimal spin was α–$\beta = 3$, and this value was used for the simulation. Then, using the calculated coordinates obtained from the calculations on the Pt 38 cluster, CD was placed on the metal as shown in Fig. 7a. The coordinates of the quinoline moiety of the alkaloid, at the edge of the Pt

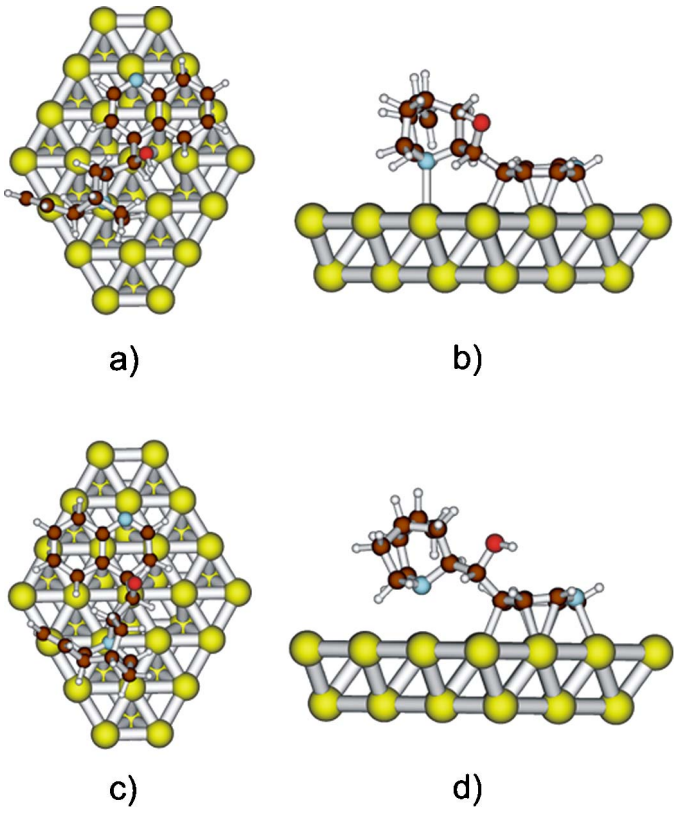

Fig. 6. Adsorption of CD on a Pt 38 cluster. Top and side views of Surface Quinuclidine Bound(1) (SQB(1)) (a–b) and Surface Quinuclidine Bound(2) (SQB(2)) (c–d). The quinuclidine moiety is chemisorbed to the metal by the tertiary nitrogen.

25 cluster, were frozen to the equilibrium values, so that edge effects should not disturb the optimal adsorption. Only the quinuclidine moiety, C(9), and its substituents (Fig. 3) were set free to optimize.

Fig. 7 presents three representative geometries taken from this simulation. The first of these shows the starting point (Fig. 7a); the second shows an intermediate point (Fig. 7b), characterized in what follows; and the third shows the final geometry (Fig. 7c). The top right graphic of Fig. 7 shows the energy profile of this transformation, while the bottom graphic shows the variation of the charges (quadrupole-derived charges [59]) on the transferred hydrogen atom and on the platinum atom to which hydrogen is bound at the beginning of the simulation. In the starting geometry (Fig. 7a), the distance between the tertiary nitrogen and the adsorbed hydrogen was 1.60 Å, whereas the distance between hydrogen and platinum (binding on a top site) was 1.58 Å. At this point, the hydrogen is bound to the cluster and bears a negative charge, whereas the platinum atom has a positive charge. At point b, corresponding to the intersect of the curves in the bottom graphic of Fig. 7, the N–H distance had shortened to 1.21 Å and Pt–H had increased to 1.83 Å (Fig. 7b). At this point, the charges are equal. When the simulation ended and the minimum was found (Fig. 7c), the hydrogen had completely migrated to bind the tertiary nitrogen and had changed its charge from negative to positive, leaving the negative charge on the metal. This transformation followed a smooth monotonic path along the reaction coordinate.

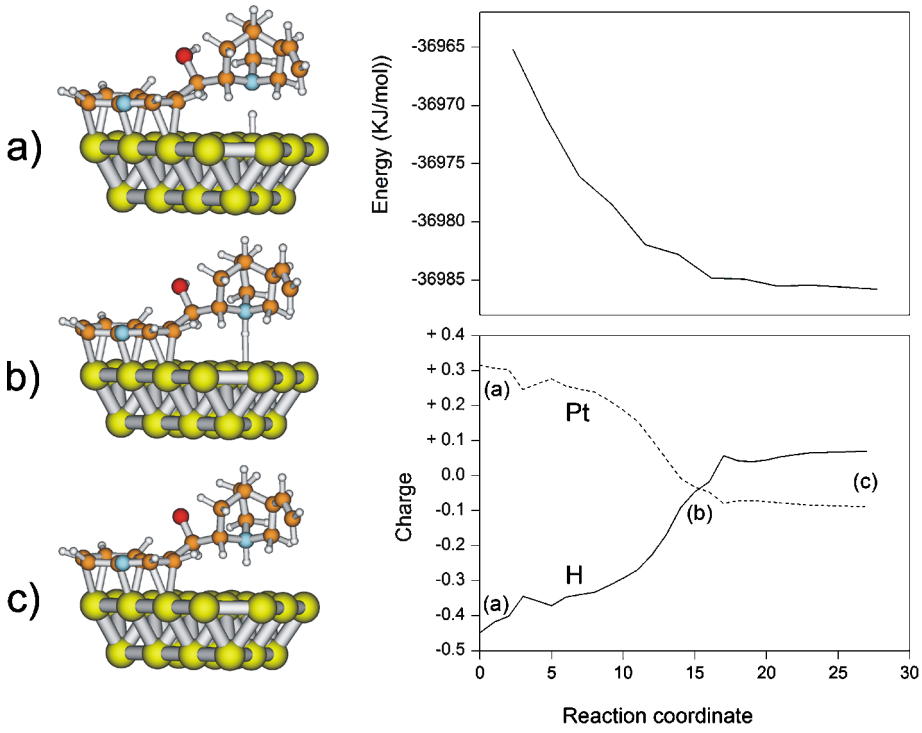

Fig. 7. Hydrogen uptake of CD from a platinum surface. The top right graphic represents the energy profile of the transfer process and shows the smooth decrease in energy from a to c. The bottom right graphic shows the behaviour of the calculated charges (Quadrupole Derived Charges) during the transfer process.

3.3. *In situ ATR-IR spectroscopy*

ATR-IR spectroscopy was used to provide experimental evidence of the proposed behavior of CD on Pt. The first point to be verified was the flexibility of the quinuclidine moiety. Infrared spectroscopy demonstrated the ability to detect adsorbed species of CD that differ depending on the orientation of the quinoline ring with respect to the metal surface [34]. Analysis of the spectra of CD on platinum alone is not sufficient to resolve the orientation of the quinuclidine moiety. Comparison with other modifiers of the cinchona family might reveal additional features. A nice example in which the quinuclidine moiety can be seen to change its spatial arrangement is given by the ATR-IR spectra of CD and *O*-phenyl-cinchonidine (PhOCD) adsorbed on Pt model films [32]. The spectra were recorded in the presence of solvent (CH_2Cl_2) and hydrogen (Fig. 8). The assignment of the signals in the 1700–1500 cm^{-1} region is known [32,34,60] and is consistent with the interaction of the quinoline ring with the metal surface. The signal at 1458 cm^{-1} corresponds to δ(C–H) deformation modes of the quinuclidine skeleton. The most striking observation is that the signal is much weaker in the case of PhOCD (b) than in the case of CD (a), in contrast with spectra in the liquid phase. To further confirm this observation, spectrum (c) shows that adsorption of CD on a surface pretreated with PhOCD results in the enhancement of this signal due to formation of a mixed chiral layer on Pt dominated by CD. This change in intensity is interpreted as a change of position of the quinuclidine moiety with respect to the surface and to the quinoline moiety [32]. Due to the critical role of the quinuclidine moiety in the enantiodiscriminating process observed for some substrates [58], this may be

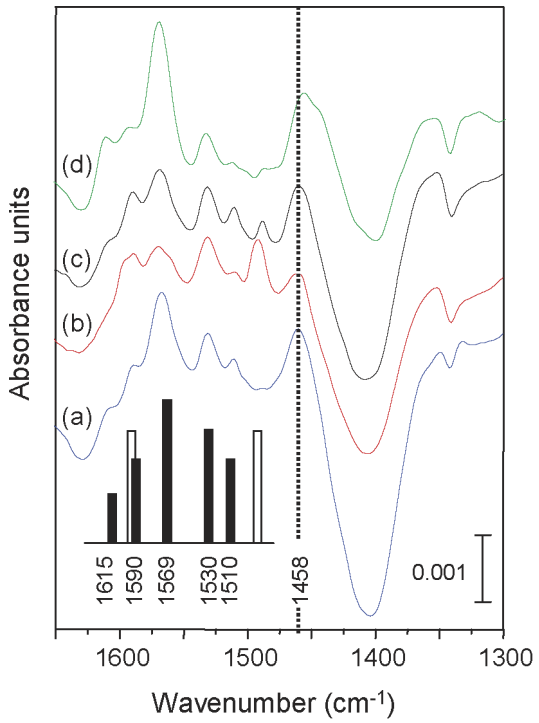

Fig. 8. ATR-IR spectra of (a) CD, (b) PhOCD and (d) CD hydrochloride adsorbed on Pt/Al_2O_3 model catalysts. Spectrum (c) corresponds to CD adsorbed on a Pt surface pre-equilibrated with PhOCD (details in Ref. [32]). The solid bars give a pictorial of the position and approximate relative intensity of the signals of the quinoline moiety typically observed on Pt. The two open bars represent the position and intensity of the additional signals of the phenyl ring of PhOCD (1598 and 1495 cm^{-1}). The negative signals at 1400 and 1339 cm^{-1} indicate removal of hydrocarbon species from the metal surface upon adsorption of the cinchona modifiers.

one cause of the inversion of enantioselectivity observed when CD replaces PhOCD as surface modifier [31].

The second aspect and the topic of the present work—obtaining experimental information on the hydrogen uptake on platinum under the conditions applied in ATR-IR measurements—is challenging. Recently, we showed that CD adsorbed on Pt interacts with ketopantolactone in toluene by formation of a hydrogen bond [54]. The presence of a signal at about 2580 cm^{-1} indicated that CD is protonated in the absence of an acidic solvent, but no information was obtained in the region of the ring-skeleton modes of quinuclidine. Fig. 8 shows the spectra of (a) CD and (d) CD hydrochloride adsorbed on Pt under identical experimental conditions. CD hydrochloride displays similar adsorption behavior to CD. Except for possible differences in the relative abundance of the adsorbed species, no important differences in the ATR-IR spectra of the two parent modifiers can be detected. This observation suggests that at the metal surface, the quinuclidine moiety of CD has the same structure as in the protonated quinuclidine of CD hydrochloride. This may mean either that the quinuclidine of CD is protonated on the surface or that the quinuclidine of CD hydrochloride is deprotonated by the surface, and the computational study here presented shows that the former process is energetically favored. Although this conclusion is tempting, further studies are needed to confirm its validity. Doubts may arise from the presence of HCl originating from CH_2Cl_2 solvent decomposition on Pt [13]. Note, however, that similar spectra were reported for CD adsorption from cyclohexane solvent [34] and that experiments are realized in a flow-through mode, which enables quick removal of nonadsorbing species.

4. Discussion

Theoretical calculations have shown that the quinuclidine moiety may contribute to the adsorption of CD on Pt. The flexibility around the τ_1 and τ_2 angles can generate conformations in which the quinuclidine-N is closer to the metal and chemically bound to it. Experimental support for this result comes from comparing the ATR-IR spectra of structurally different surface modifiers, which shows that the intensity of the signals due to the quinuclidine moiety can be strikingly different. CD and PhOCD, although having almost identical quinoline adsorption patterns [32], differ in terms of the intensity of quinuclidine bands. This variation can be interpreted as a change in population of the conformers generated by rotation of this moiety. Conformations of adsorbed CD in which the quinuclidine is close to the surface have also been found in a classical molecular dynamics study of the adsorption of CD on platinum [61]. In this work, due to the classical Hamiltonian used, the adsorption energies were underestimated, whereas the Pt–C bond distances were up to 50% longer than those found with quantum chemical methods [35,62,63], but the results are in excellent qualitative agreement with our findings. More convincing experimental evidence of the conformational flexibility of quinuclidine moiety comes from STM data on the adsorption and mobility of CD on a Pt(111) surface [64]. One of the adsorbed species was found to be conformationally sensitive to the STM tip, attributed to the flexibility of the quinuclidine. It was also observed that introducing hydrogen on the platinum surface increased the mobility of the alkaloid. This is indeed consistent with the partial hydrogenation of the quinoline ring [65,66], and also with the surface-mediated protonation of the quinuclidine moiety, which leads to the loss of an anchoring point of the alkaloid to the surface. The calculations also show that CD can be protonated by the surface hydrogen. Analysis of the surface spectra of adsorbed CD and its hydrochloride might suggest the experimental evidence for this process. The implications of this behavior are related to the interpretation of the reaction mechanism of the enantioselective hydrogenation of activated ketones on cinchona-modified supported Pt catalysts. It had been proposed that the promoter of hydrogen transfer should be a protonated CD molecule when the reaction is performed in acetic acid as a solvent. But the reaction occurs with little loss of enantioselectivity (and in some cases with higher rate) with toluene as the solvent [65], although in this case a protonation of the CD did not seem possible on the basis of the classical standpoint of acid-base reactivity in solution, although it has been reported spectroscopically [54]. In the literature this inconsistency had been overcome by calling in existence a half-hydrogenated state of the reactant, able to interact with the tertiary nitrogen of quinuclidine through a hydrogen-nitrogen interaction [67]. The present results show that the half-hydrogenated state is unnecessary for a consistent reaction mechanism in which a hydrogen bond is formed between the quinuclidine tertiary nitrogen and the adsorbed activated ketone. The hydrogen necessary for the formation of the H-bond could be picked up by the quinuclidine-N from the surface, forming an ammonium ion also in the absence of a classic acidic medium, because the hydrogen-rich surface is able to deliver a proton to the alkaloid. Also note that in the case of dihydrogen, the nitrogen-promoted charge separation is bound to generate a hydride that can readily react as a nucleophile with the keto-carbonyl. This viewpoint can explain the amine-mediated rate acceleration observed for these catalysts [4,53]. In general, a charge separation can have catalytic implications (e.g., acid catalyzed nucleophilic additions to ketones). A more formal interpretation scheme is that obtained by second-order perturbation theory, from which it can be derived that the lowest reaction pathway can be (approximately) determined by either the charge on the reactants (charge-controlled mechanism) or by orbital superposition (orbital-controlled mechanism) [68]. Here we have shown that protonation generates charge separation and thus can give rise to a charge-controlled lowering of the barrier. We have shown elsewhere that protonation can give rise to orbital-controlled lowering of the barrier (although the model used neglected the effect of the surface) [51,52]. Interestingly, both effects are acting in the same direction. From a mechanistic standpoint, another important consequence follows. Protonation of CD irrespective of the solvent used as reaction medium implies that the nucleophilic activity of the tertiary nitrogen is hindered under catalytic conditions, and calls into question those hypotheses of reaction mechanisms that imply a nucleophylic attack of the quinuclidine nitrogen to the keto-carbonyl [69–72]. Considering the literature that has

been dedicated to the topic of the adsorption of CD on platinum [34,73,74], the picture that results is that of a dynamic equilibrium of differently adsorbed species, either weakly (tilted) or strongly bound (flat) to the metal. Under catalytic conditions (6.8 μmol in 5 ml solvent in standard hydrogenation reactions), CD species in tilted and flat orientation compete for adsorption on platinum, and those with the quinoline ring parallel to the metal surface are more strongly adsorbed. These latter species also allow for rotation of the τ_1 angle, which brings the quinuclidine near to the surface, incidentally also allowing for hydrogenation of the C(10)=C(11) double bond. The conformational freedom around the angles τ_1 and τ_2 allows the interaction of quinuclidine with the hydrogen-rich metal via the tertiary nitrogen. This could therefore be protonated by the surface, generating a charge separation, as shown in Fig. 7. Hydrogen exchange between the alkaloid and the surface could trigger an ionic mechanism of hydrogenation based on the interaction between a protonated quinuclidine and the oxygen atom of the keto-carbonyl moiety of an activated ketone, with a successive income of a hydride to the carbon of the same moiety. This would explain the feasibility of the hydrogenation with a 1:1 mechanism proposed by Baiker and coworkers [8,75] when aprotic solvents, such as toluene, are used. The role of the solvent would be restricted to the conformational bias set to a flexible modifier, thus affecting enantioselectivity, and to competition with the modifier for surface sites, whereas the acid-base properties would be preferentially mediated by the metal, acting as the proton donor to the quinuclidine.

5. Conclusions

The combined theoretical and spectroscopic investigation of CD adsorption adds further insight into the long-debated problem of the adsorption and action of surface modifiers in the enantioselective hydrogenation of activated ketones on cinchona modified platinum. In particular, the complete CD was calculated on a large metal cluster and the role of the quinuclidine moiety as part of the anchoring group could be established when hydrogen is not present on the surface. Thus, under nonreducing conditions, the anchoring of the alkaloid is based not only on the quinoline moiety, but also on the quinuclidine moiety. Furthermore, it has been shown that the tertiary nitrogen is able to remove a proton from the surface, generating a charge separation. This interprets the often-observed similar behavior, in terms of enantioselectivity, of the catalyst in acidic solvents (e.g., AcOH) and aprotic solvents (e.g., toluene). In both cases protonation of the CD can occur, mediated either by the solvent or by the surface. Within this framework, the 1:1 interaction model is consistent with all observations and does not require the hypothesis of the formation of a half-hydrogenated state of the substrate. Rate acceleration is interpreted with the ability of the tertiary amine to activate the surface hydrogen, promoting hydrogen transfer and the availability of H$\delta+$ and H$\delta-$ hydrogen species in proximity of the surface. Furthermore, it is noted that a protonated quinuclidine nitrogen also in aprotic solvents is inconsistent with mechanisms based on the hypothesis of a nucleophilic attack of the quinuclidine-N atom on the activated keto-carbonyl group.

Acknowledgments

Computing time was provided by the ETH Zurich and by the Swiss Center for Scientific Computing (CSCS) in Manno. Financial support from the Swiss National Foundation is gratefully acknowledged.

References

[1] D.Y. Murzin, P. Mäki-Arvela, E. Toukoniitty, T. Salmi, Catal. Rev. 47 (2005) 175.
[2] T. Bürgi, A. Baiker, Acc. Chem. Res. 37 (2004) 909.
[3] M. Studer, H.U. Blaser, C. Exner, Adv. Synth. Catal. 345 (2003) 45.
[4] A. Baiker, H.U. Blaser, in: G. Ertl, H. Knözinger, J. Weitkamp (Eds.), Handbook of Heterogeneous Catalysis, vol. 5, VCH, Weinheim, Germany, 1997, p. 2422.
[5] G.J. Hutchings, Catal. Lett. 75 (2001) 1.
[6] N. Künzle, R. Hess, T. Mallat, A. Baiker, J. Catal. 186 (1999) 239.
[7] P.B. Wells, A.G. Wilkinson, Top. Catal. 5 (1998) 39.
[8] A. Baiker, J. Mol. Catal. A 115 (1997) 473.
[9] B. Török, K. Felfoldi, G. Szakonyi, K. Balázsik, M. Bartók, Catal. Lett. 52 (1998) 81.
[10] M. Schürch, N. Künzle, T. Mallat, A. Baiker, J. Catal. 176 (1998) 569.
[11] W.A.H. Vermeer, A. Fulford, P. Johnston, P.B. Wells, Chem. Commun. (1993) 1053.
[12] J.A. Slipzenko, S.P. Griffiths, P. Johnston, K.E. Simons, W.A.H. Vermeer, P.B. Wells, J. Catal. 179 (1998) 267.
[13] E. Toukoniitty, P. Mäki-Arvela, M. Kuzma, A. Villela, A.K. Neyestanaki, T. Salmi, R. Sjöholm, R. Leino, E. Laine, D.J. Murzin, J. Catal. 204 (2001) 281.
[14] E. Toukoniitty, P. Mäki-Arvela, J. Kuusisto, V. Nieminen, J. Paivarinta, M. Hotokka, T. Salmi, D.Y. Murzin, J. Mol. Catal. A 192 (2003) 116.
[15] O.J. Sonderegger, T. Bürgi, A. Baiker, J. Catal. 215 (2003) 116.
[16] B. Török, K. Felföldi, K. Balázsik, M. Bartók, Chem. Commun. (1999) 1725.
[17] M. Studer, S. Burkhardt, H.U. Blaser, Chem. Commun. (1999) 1727.
[18] M. Bodmer, T. Mallat, A. Baiker, in: F.E. Herkes (Ed.), Catalysis in Organic Reactions, Marcel Dekker, New York, 1998, p. 75.
[19] M. von Arx, T. Mallat, A. Baiker, J. Catal. 193 (2000) 161.
[20] K. Balázsik, B. Török, K. Felfoldi, M. Bartók, Ultrason. Sonochem. 52 (2001) 149.
[21] M. von Arx, T. Mallat, A. Baiker, Tetrahedron: Asym. 12 (2001) 3089.
[22] M. von Arx, T. Mallat, A. Baiker, Catal. Lett. 78 (2002) 267.
[23] G.-Z. Wang, T. Mallat, A. Baiker, Tetrahedron: Asym. 8 (1997) 2133.
[24] A. Szabó, N. Künzle, T. Mallat, A. Baiker, Tetrahedron: Asym. 10 (1999) 61.
[25] A. Szabó, N. Künzle, M. Schürch, G.-Z. Wang, T. Mallat, A. Baiker, Chem. Commun. (1998) 1377.
[26] W.R. Huck, T. Mallat, A. Baiker, J. Catal. 193 (2000) 1.
[27] W.R. Huck, T. Mallat, A. Baiker, New J. Chem. 6 (2002) 26.
[28] M. Maris, W.R. Huck, T. Mallat, A. Baiker, J. Catal. 219 (2003) 52.
[29] K. Szöri, G. Szöllosi, K. Felföldi, M. Bartók, React. Kinet. Catal. Lett. 84 (2005) 151.
[30] A. Baiker, J. Mol. Catal. A 115 (1997) 473.
[31] S. Diezi, T. Mallat, A. Szabo, A. Baiker, J. Catal. 228 (2004) 162.
[32] N. Bonalumi, A. Vargas, D. Ferri, T. Bürgi, T. Mallat, A. Baiker, J. Am. Chem. Soc. 127 (2005) 8467.
[33] A. Baiker, Catal. Today 100 (2005) 159.
[34] D. Ferri, T. Bürgi, J. Am. Chem. Soc. 123 (2001) 12074.
[35] A. Vargas, T. Bürgi, A. Baiker, J. Catal. 226 (2004) 69.
[36] A. Vargas, T. Bürgi, A. Baiker, J. Catal. 222 (2004) 439.

[37] E.J. Baerends, J. Autschbach, A. Berces, C. Bo, P.M. Boerrigter, L. Cavallo, D.P. Chong, L. Deng, R.M. Dickson, D.E. Ellis, L. Fan, T.H. Fischer, C. Fonseca Guerra, S.J.A. van Gisbergen, J.A. Groeneveld, O.V. Gritsenko, M. Gröning, F.E. Harris, P. van den Hoek, H. Jacobsen, G. van Kessel, F. Kootstra, E. van Lenthe, V.P. Osinga, S. Patchkovskii, P.H.T. Philipsen, D. Post, C.C. Pye, W. Ravenek, P. Ros, P.R.T. Schipper, G. Schreckenbach, J.G. Snijders, M. Sola, M. Swart, D. Swerhone, G. te Velde, P. Vernooijs, L. Versluis, O. Visser, E. van Wezenbeek, G. Wiesenekker, S.K. Wolff, T.K. Woo, and T. Ziegler, ADF—Amsterdam Density Functional, Release 2004.1, Scientific Computing and Modelling NV, Vrije Universiteit; Theoretical Chemistry, Amsterdam.
[38] M. Saeys, M.-F. Reyniers, G.B. Marin, M. Neurock, J. Phys. Chem. 106 (2002) 7489.
[39] P.H.T. Philipsen, E. vanLenthe, J.G. Snijders, E.J. Baerends, Phys. Rev. B 56 (1997) 13556.
[40] G. Pacchioni, S.C. Chung, S. Kruger, N. Rosch, Surf. Sci. 392 (1997) 173.
[41] E. van Lenthe, E.J. Baerends, J.G. Snijders, J. Chem. Phys. 99 (1993) 4597;
E. van Lenthe, E.J. Baerends, J.G. Snijders, J. Chem. Phys. 101 (1994) 9783;
E. van Lenthe, E.J. Baerends, J.G. Snijders, J. Chem. Phys. 105 (1996) 6505;
E. van Lenthe, R. van Leeuwen, E.J. Baerends, J.G. Snijders, Int. J. Quantum Chem. 57 (1996) 281;
E. van Lenthe, E.J. Baerends, J.G. Snijders, J. Chem. Phys. 110 (1999) 8943.
[42] J.G. Snijders, E.J. Baerends, P. Ros, Mol. Phys. 38 (1979) 1909.
[43] G. te Velde, F.M. Bickelhaupt, E.J. Baerends, C. Fonseca Guerra, S.J.A. Van Gisbergen, J.G. Snijders, T. Ziegler, J. Comput. Chem. 22 (2001) 931.
[44] S.H. Vosko, L. Wilk, M. Nusair, Can. J. Phys. 58 (1980) 1200.
[45] A.D. Becke, Phys. Rev. A 38 (1988) 3098.
[46] J.P. Perdew, Phys. Rev. B 33 (1986) 8822.
[47] G.A. Somorjai, Introduction to Surface Chemistry and Catalysis, Wiley, New York, 1994.
[48] G. Schaftenaar, J.H. Noordik, J. Comput.-Aided Mol. Design 14 (2000) 123.
[49] D. Ferri, T. Bürgi, A. Baiker, J. Phys. Chem. B 105 (2001) 3187.
[50] D. Ferri, T. Bürgi, A. Baiker, J. Phys. Chem. B 108 (2004) 14384.
[51] A. Vargas, T. Bürgi, A. Baiker, New J. Chem. 26 (2002) 807.
[52] A. Vargas, T. Bürgi, M. von Arx, R. Hess, A. Baiker, J. Catal. 20 (2002) 489.
[53] H.U. Blaser, H.P. Jalett, D.M. Monti, J.F. Reber, J.T. Wehrli, Stud. Surf. Sci. Catal. 41 (1988) 153.
[54] N. Bonalumi, T. Bürgi, A. Baiker, J. Am. Chem. Soc. 125 (2003) 13342.
[55] G.D.H. Dijkstra, R.M. Kellogg, H. Wynberg, J.S. Svendsen, I. Marko, B. Sharpless, J. Am. Chem. Soc. 111 (1989) 8069.
[56] G.D.H. Dijkstra, R.M. Kellogg, H. Wynberg, J. Org. Chem. 55 (1990) 6121.
[57] T. Bürgi, A. Baiker, J. Am. Chem. Soc. 120 (1998) 12920.
[58] H.U. Blaser, H.P. Jalett, D.M. Monti, A. Baiker, J.T. Wehrli, Stud. Surf. Sci. Catal. 67 (1991) 147.
[59] M. Swart, P.T. Van Duijnen, J.G. Snijders, J. Comput. Chem. 22 (2001) 79.
[60] W. Chu, R.J. Le Blanc, C.T. Williams, J. Kubota, F. Zaera, J. Phys. Chem. B 107 (2003) 14365.
[61] S.R. Calvo, R.J. Le Blanc, C.T. Williams, P.B. Balbuena, Surf. Sci. 563 (2004) 57.
[62] M. Saeys, M.-F. Reyniers, G.B. Marin, J. Phys. Chem. B 106 (2002) 7489.
[63] P.R.N. de Souza, D.A.G. Aranda, J.W. de Carneiro, C. da S.B. de Oliveira, O.A.C. Antunes, F.B. Passos, Int. J. Quantum Chem. 92 (2003) 400.
[64] M. von Arx, M. Wahl, A. Jung, A. Baiker, Phys. Chem. Chem. Phys. 7 (2005) 273.
[65] H.U. Blaser, H.P. Jalett, W. Lottenbach, M. Studer, J. Am. Chem. Soc. 122 (2001) 12675.
[66] M. Bartók, T. Bartók, G. Szöllösi, K. Felföldi, Catal. Lett. 61 (1999) 57.
[67] G. Bond, P.A. Meheux, A. Ibbotson, P.B. Wells, Catal. Today 19 (1991) 371.
[68] A. Devaquet, Mol. Phys. 18 (1970) 233.
[69] R.L. Augustine, S.K. Taneilyan, L.K. Doyle, Tetrahedron: Asym. 4 (1993) 1803.
[70] G. Vayner, K.N. Houk, Y.-K. Sun, J. Am. Chem. Soc. 126 (2004) 199.
[71] K. Balázsik, M. Bartók, J. Catal. 224 (2004) 463.
[72] M. Bartók, M. Sutyinszki, K. Balázsik, G. Szöllösi, Catal. Lett. 100 (2005) 161.
[73] J. Kubota, F.J. Zaera, J. Am. Chem. Soc. 123 (2001) 11115.
[74] W. Chu, R.J. LeBlanc, C.T. Williams, Catal. Commun. 3 (2002) 547.
[75] O. Schwalm, J. Weber, B. Minder, A. Baiker, Catal. Lett. 23 (1994) 271.